BNL--21888
CONF-761006--27
BNL# 21888

To be published in
IEEE Trans. Nucl. Sci.

Presented at IEEE Nuclear Science
Symposium, 20-22 October 1976
Braniff Place Hotel, New Orleans

FLAT HELICAL DELAY LINES FOR POSITION READOUT ALONG THE ANODE WIRE IN MWPC AND DRIFT CHAMBERS*

H. Okuno,† R. L. Chase,
J. Fischer, and A. H. Walenta‡

October 1976

*Research carried out under the auspices of Energy Research and Development Administration: Contract No. EY-76-C-02-0016.

†On leave from Institute for Nuclear Study, University of Tokyo, Tanashi, Tokyo, Japan.

‡On leave from University of Heidelberg, Heidelberg, Germany.

DISCLAIMER

FLAT HELICAL DELAY LINES FOR POSITION READOUT ALONG THE ANODE WIRE IN MWPC AND DRIFT CHAMBERS*

H. Okuno,† R. L. Chase,
J. Fischer, and A. H. Walenta‡

Brookhaven National Laboratory
Upton, New York 11973

Abstract

Simple, flat helical delay lines were developed for avalanche position determination along each anode wire, for unambiguous readout of multiparticle events in multiwire drift or proportional chambers.

Lines of various propagation delay and dimensions were tested with x-rays and β-rays in several gas mixtures. Avalanche position resolutions of 0.2 mm and 0.6 mm FWHM, respectively, were obtained with a line 30 cm long in non electron-attaching gases.

Introduction

Delay line readout of the avalanche position in multiwire proportional and drift chambers is now in common use.[1-8] In most of these applications, the positions of the avalanches are projected on two orthogonal delay lines for two dimensional readout. If more than one particle is present, the readout is ambiguous and requires additional coordinate readout. In experiments with very high energy particles, an efficient detection of multiparticle events has become more important.

The unambiguous, two dimensional position determination of several simultaneous particles in a single chamber can be accomplished by avalanche position readout along each anode wire. At least two methods have been developed for this purpose: charge division using a resistive anode wire[9] or delay line readout of the induced signal in the proximity of and along the anode wire.[6,8] Breskin et al.[6] and Atac et al.[8] applied the latter method to the drift chamber with a small helix or a thin strip line between two anode wires. Because of the high signal velocity of the lines, the reported spatial resolution is limited to 2-6 mm FWHM along the anode wire.

Here we report on delay lines which are simple to make and apply, and result in good spatial resolution.

Delay Line

The structure of the delay line and its position on a MWPC are shown in Fig. 1. The delay line consists of a wire helix wound around a thin plastic strip. A narrow straight ground conductor is cemented to one exterior surface.

Characteristic properties of the line depend largely on the geometry. Typical lines investigated are shown in Table 1. The length of the line is about 30 cm. Three kinds of cross sections of the core strip were tested: 14.3 x 1.6 mm^2, 14.3 x 0.8 mm^2 and 25.4 x 1.6 mm^2. The windings ranged from 11 to 38 turns/cm, with wire diameters of 75, 100 and 125 μm. Characteristic impedances and specific propagation delays are in the region between 270 and 1000 Ω, and between 1.3 and 8 ns/cm, respectively.

The geometry of the line, within the constraints of low mass and limited width, permits simple construction without the need for phase compensation. The decrease of the effective inductance for high frequency components of the signal is relatively small because of the distance between the turns and the small thickness of the line. The relatively small width of the ground strip increases the L/C ratio and thus the characteristic impendance. It also improves the coupling efficiency of the signal to the coil relative to the ground strip. The coupling efficiency is also enhanced by locating the ground strip on the side away from the chamber.

Attenuation of the signal along the total length of the line, 30 cm, is less than 10%, and is due to the ratio of total resistance and characteristic impendance. The total delay-to-rise time ratio is around 6.

Experimental Arrangements

The performance of the line was tested with a MWPC having a full gap of 12.7 mm, and anode wires of 25 μm in diameter spaced 6.35 mm. As is shown in Fig. 1, the delay line under test can be placed on the outside of one cathode plane, which is made of a Mylar film with a resistive coating on the inside under the delay line. The resistance of the coating is about 10^6 - 10^7 Ω per square. This permits easy interchange of delay lines and does not interfere with the internal DC field of the chamber. A charge signal corresponding to the anode avalanche is induced on the line through the resistive cathode plane. The induced charge is normally shared by nearby conductors, and these conductors were simulated by external plates or internal metal coatings located within 1.5 mm along each side of the delay line.

Each end of the line is coupled to a charge sensitive preamplifier whose input constitutes an electronically cooled termination[10] for noise reduction. Signals are processed by timing filter amplifiers (ORTEC 454) and constant fraction discriminators (ORTEC 473) as shown in the block diagram of Fig. 2. The time constants of the electronic system are optimized to fit the signal rise time from the line.

The measurement of the spatial resolution was made in two configurations; (a) the line was placed over and parallel to the anode wire as would be the

*Research carried out under the auspices of Energy Research and Development Administration: Contract No. EY-76-C-02-0016.

†On leave from Institute for Nuclear Study, University of Tokyo, Tanashi, Tokyo, Japan.

‡On leave from University of Heidelberg, Heidelberg, Germany.

case in most applications, and (b) the line was placed orthogonal to the anode wire. With the latter arrangement, one can measure the intrinsic spatial resolution of the delay line readout. With the arrangement (a), the spatial spread of the primary ionization due to the source size and collimation and range of the charged particle, worsen the spatial resolution. Therefore most tests were made with the arrangement (b). Results with the arrangement (a) after correction for the above factors were similar to results with the arrangement (b).

Results for X-rays and β-rays

The spatial resolution for ^{55}Fe x-rays was studied with two gas mixtures: A(90%) + CH_4(10%) and A(80%) + CO_2(20%). The avalanche size was measured on the anode wire. For these gases and essentially point ionization, the proportional region extends to 2 x 10^6 electrons measured with 1 μs clipping time of the anode signal. With bigger avalanches the signal amplitude versus the amount of primary ionization and applied field starts to saturate. Reignition[14] becomes noticeable at avalanche sizes over ~ 2 x 10^7 electrons. The maximum avalanche size obtained without reignition is two times bigger for A(80%) + CO_2(20%) than for A(90%) + CH_4(10%).

Spatial and time resolution versus avalanche size for ^{55}Fe x-rays with a typical delay line, #10, are shown in the upper curve of Fig. 3. The resolution with a pulser signal capacitively coupled with a point probe located in the proximity of the line is also shown to indicate the effect of any noise or non-linearity from the avalanche process on the resolution. For these measurements, the pulser signal was shaped like the x-ray signal. Results with x-rays and pulser signals are very close up to an avalanche size of ~10^7 electrons and then separate at bigger avalanche sizes. This difference may stem from instabilities in the avalanche process in this region.

The middle curve shows the resolutions with the delay line with the pulser injected into the parallel connected preamp inputs to indicate the noise contribution from the delay line. The bottom curve is taken without preamplifiers to indicate the noise from these. The data show that the noise contributions to the resolution from this delay line is about equal to that from the preamplifiers in absolute value.

The dependence of the spatial resolution $\Delta\ell/\ell$ on the anode avalanche size Q_A can be deduced empirically from the straight part of the corresponding curve of Fig. 3 as $\Delta\ell/\ell \propto Q_A^{-0.9}$. According to the noise analysis by Radeka[10], $\Delta\ell/\ell$ can be stated as

$$\frac{\Delta\ell}{\ell} = 2.46 \frac{1}{\Theta_D} \cdot \frac{e_n}{Z_0 Q_s} \cdot t_{FW}^{\frac{1}{2}} \quad [\text{FWHM}], \qquad (1)$$

where Θ_D is the ratio of the total delay to the signal rise time from the delay line, Z_0 is the line impedance, t_{FW} is the FWHM of the output pulse in response to a δ-function input, Q_s is the signal charge at the end of the line and e_n is an equivalent series noise voltage of the amplifier for cooled terminations. For this line #10, $\Theta_D \simeq 6.3$, $Z_0 \simeq 700\ \Omega$ and $t_{FW} \simeq 25$ ns. The measured spatial resolution $\Delta\ell/\ell$ is 2.2 x 10^{-3} at an anode avalanche size of 5 x 10^6 electrons. Without delay line, the equivalent resolution is ≃ 1.4 x 10^{-3} for the same avalanche size. The effective avalanche size on the delay line is much smaller than the anode avalanche size because the anode avalanche size is measured with a clipping time of 1 μs; while the signal shaping differentiation time constant used on the delay line signal is only 20 ns, and because the coupling efficiency of the line to the avalanche is about 30%. As a whole, since only about 10% of the anode signal is used for the time measurements, Q_s the effective charge into the line is only about 5 x 10^5 electrons. From these data, the preamplifier and delay line noise combined is estimated as $e_n \simeq 2 \times 10^{-9}$ V/$Hz^{\frac{1}{2}}$.

The spatial resolutions with different delay lines are summarized in Fig. 4 as a function of the specific propagation delay t_D. In the region of t_D between 1.3 and 8 ns/cm, the spatial resolution varies almost linearly as $1/t_D$ for a given avalanche size on the anode for all lines. This means that the time resolution is nearly constant for all lines because $\Delta t = \Delta\ell \cdot t_D$. This behavior is due to the similar construction of the delay lines except for the number of turns. Consequently the increase of the rise time with the slower lines is here compensated by the increase of Z_0 resulting in an improved signal to noise ratio.

The resolution for minimum ionizing particles passing through the chamber measured with ^{106}Ru β-rays is shown in Fig. 5. In these measurements, the delay line pulses were shaped by 20 ns differentiation. The large difference in the resolution between β-rays and x-rays is due to the different rise time of the chamber signal. The drift time of electrons liberated along the particle track increases the width of the current signal for β-rays up to 150 ~ 250 ns, depending on the gas mixtures and applied field. These delay lines are not optimized for such slow signals. The differentiated signal used for fast timing utilizes only a fraction of the total induced charge. The best spatial resolution for β-rays was obtained with the differentiation time constant of 20 - 50 ns. The gas mixture with a faster electron drift velocity gave a better spatial resolution for the same anode avalanche size, which was confirmed with pure CH_4, a much faster gas. Unfortunately this gas requires a high operating voltage.

These lines can also be useful for high precision measurements of avalanche location over limited distances. In order to get an idea of the resolving power of such a line, a short line, 25.4 mm wide, 1.6 mm thick, 6 cm long, 104 turns/25.4 mm, t_D = 16ns/cm and $Z_0 \simeq 1000\ \Omega$, was put on the cathode plane orthogonal to the anode wire. With a gas mixture of A(80%) + CO_2(20%), the resolution of 85 μm FWHM at an avalanche size of 2 x 10^7 electrons permitted determination of an effective avalanche location relative to the anode wire. In Fig. 6, the effective position of the avalanche was measured for two different source positions on each side of the anode wire. Two distinct locations were found indicating that the avalanche does not surround the wire uniformly but the measured location, left or right, indicates on which side the avalanche started. The distance between two peaks was 190 μm.

Indications of avalanche position asymmetry have been reported by Walenta *et al.*[11] in a drift chamber, and Charpak and Sauli[12] in a MWPC using the ratio of induced charges on cathode strips. The effect of avalanche localization on one side of the wire has been confirmed with other methods and will be reported elsewhere.[13]

Conclusion

With the simple, flat delay line, it is shown that the avalanche position can be measured with good precision. Spatial resolutions of 0.2 mm FWHM and

0.6 mm FWHM were obtained for ^{55}Fe x-rays and β-rays, respectively, with the line of $t_D \simeq 5$ ns/cm at an avalanche size of 2×10^7 electrons.

Compared to the printed delay line[7] at the same distance from the anode wire and for the same avalanche size, this line gives better spatial resolution because of (1) its efficient coupling to the anode, (2) its higher impedance and (3) its slower propagation velocity. However, the thickness of our line is somewhat greater (radiation length of 1.6 mm Lucite = 4.6×10^{-3}) than that of the printed lines.

Parameters of the present delay line can be tailored to the requirement of the application. As these lines are placed outside of the chamber without disturbing the electric field inside, one has more flexibility in the choice of delay line parameters. For long, slower lines, phase compensation with small patch strips may improve the line characteristics.

Higher quality delay lines have been coupled to an entire plane of cathode wires,[1,4,5] but they can not resolve the ambiguity for multiparticle events with a single chamber. However with the use of a number of the lines here described, each associated with one or few anode wires, an unambiguous, two dimensional readout of multiparticle events becomes possible. When the present line is applied to a drift chamber, the drift time measurement on the anode wire, in addition to the separate time measurement of the signal arriving at each end of the delay line, permits us to handle two particles in a single drift space with limited precision, provided that the pulses are sufficiently separated to be resolved by the electronics.

References

1. R. Grove, I. Ko, B. Leskovar and V. Perez-Mendez, Nucl. Instr. & Meth., 99 (1972) 381.
2. D. M. Lee, S. E. Sabotka and H. A. Thiessen, Nucl. Instr. & Meth., 104 (1972) 179, 109 (1973) 421.
3. J. R. Gilland and J. E. Emming, Nucl. Instr. & Meth. 104 (1972) 241.
4. J. L. Lacy and R. S. Lindsay, Nucl. Instr. & Meth., 119, (1974) 483.
5. E. Beardsworth, J. Fischer, S. Iwata, M. J. LeVine, V.Radeka and C. E. Thorn, Nucl. Instr. & Meth., 127 (1975) 29.
6. A. Breskin, G. Charpak, F. Sauli and J. C. Santiard, Nucl. Instr. & Meth. 119 (1974) 1.
7. R. Bosshard, R. L. Chase, J. Fischer, S. Iwata and V. Radeka, IEEE Trans. Nucl. Sci. NS-22 (1975) 2053.
8. M. Atac, R. Bosshard, S. Erhan and P. Schlein, contribution to this conference.
9. J. Fischer, J. Fuhrmann, S. Iwata, R. Palmer and V. Radeka, Nucl. Instr. & Meth. 136 (1976) 19.
10. V. Radeka, IEEE Trans, Nucl. Sci. NS-21 (1974) 51.
11. A. H. Walenta, J. Heintze and B. Schürlein, Nucl. Instr. & Meth. 92 (1971) 373.
12. G. Charpak and F. Sauli, CERN 73-4 (1973).
13. J. Fischer, H. Okuno and A. H. Walenta, to be published.
14. Reignition - the appearance of small secondary avalanches produced by electrons from photoelectric effects of the first avalanche on the cathodes.

Line No.	Core Cross Section		Width of Ground Strip c(mm)	Length ℓ(cm)	Turns per 2.54cm	Wire Diameter (μm)	Characteristic Impedance $Z_0(\Omega)$	Ohmic Resistance per 30 cm R (Ω)	Propagation Delay (ns/cm)	Rise Time with pulser (ns)	Attenuation per 30 cm (%)
	Width, a (mm)	Thickness b (mm)									
1	14.3	1.6	3.2	30.0	28	75	330	36	1.29	8	< 10
2	14.3	1.6	3.2	30.5	36	75	400	45	1.79	9	< 10
3	14.3	1.6	3.2	30.0	44	75	430	58	2.23	10	< 10
4	14.3	1.6	3.2	30.5	64	100	750	51	3.20	15	< 5
5	14.3	1.6	3.2	28.0	96	100	1000	73	4.72	20	< 10
6	14.3	0.8	3.2	32.0	36	75	270	52	1.65	10	< 5
7	14.3	0.8	3.2	34.5	44	75	400	66	1.80	10	< 10
8	14.3	0.8	3.2	34.0	96	125	720	56	4.88	30	< 5
9	25.4	1.6	4.8	35.4	32	100	530	51	2.40	17	< 5
10	25.4	1.6	4.8	34.0	64	100	700	97	5.28	25	< 15

Table 1. Mechanical and Electrical Parameters of Delay Lines

Figure Captions

Fig. 1 Structure of the delay line and its position on a MWPC.

Fig. 2 Block diagram of the readout electronics.

Fig. 3 Time and spatial resolutions vs anode avalanche size for ^{55}Fe x-rays. Delay line #10, t_D = 5.28 ns/cm, was placed orthogonal to the anode wire. Gas: A(90%) + CH_4(10%). The effect of the noise contribution by the delay line and the electronic system is indicated by the difference between curves.

Fig. 4 Spatial resolution as a function of the specific propagation delay for various avalanche size and for ^{55}Fe x-rays. The lines were placed orthogonal to the anode wire. Gas: A(90%) + CH_4(10%).

Fig. 5 Spatial resolution vs anode avalanche size for β-rays passing through the chamber and for ^{55}Fe x-rays. Delay line #4, t_D = 3.20 ns/cm, was placed orthogonal to the anode wire. Anode avalanche size was measured with a 1 μsec clipping time. The delay line pulses were shaped by 20 nsec differentiation.

Fig. 6 Position spectrums of the avalanche for the two positions of the ^{55}Fe x-ray source at 2.5 mm from the anode wire. Gas: A(80%) + CO_2(20%). The spatial resolution was 85 μm FWHM and the distance between the peaks was 190 μm.

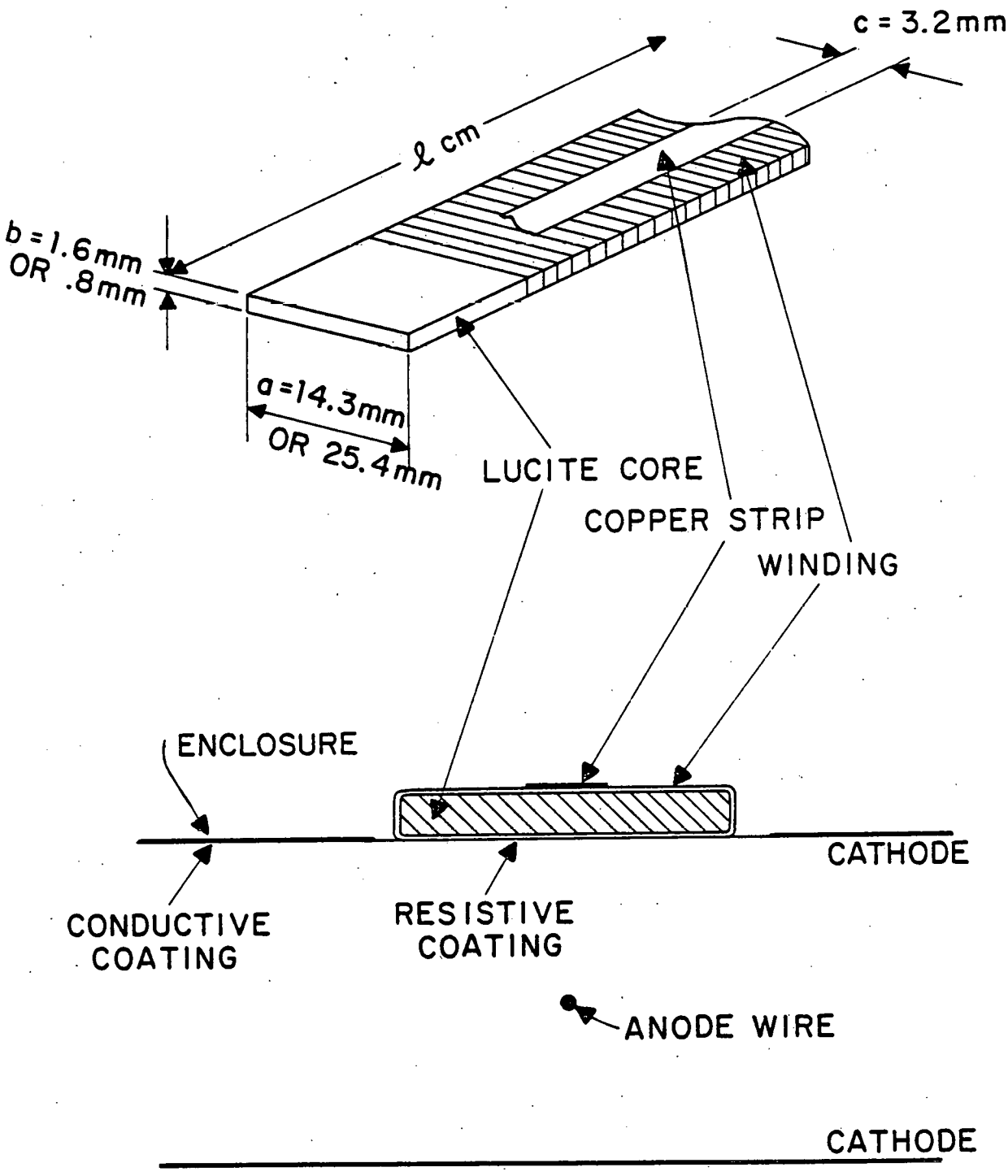
c = 3.2mm
ℓ cm
b = 1.6mm
OR .8mm
a = 14.3mm
OR 25.4mm
LUCITE CORE
COPPER STRIP
WINDING
ENCLOSURE
CATHODE
CONDUCTIVE
COATING
RESISTIVE
COATING
ANODE WIRE
CATHODE

FIGURE 1

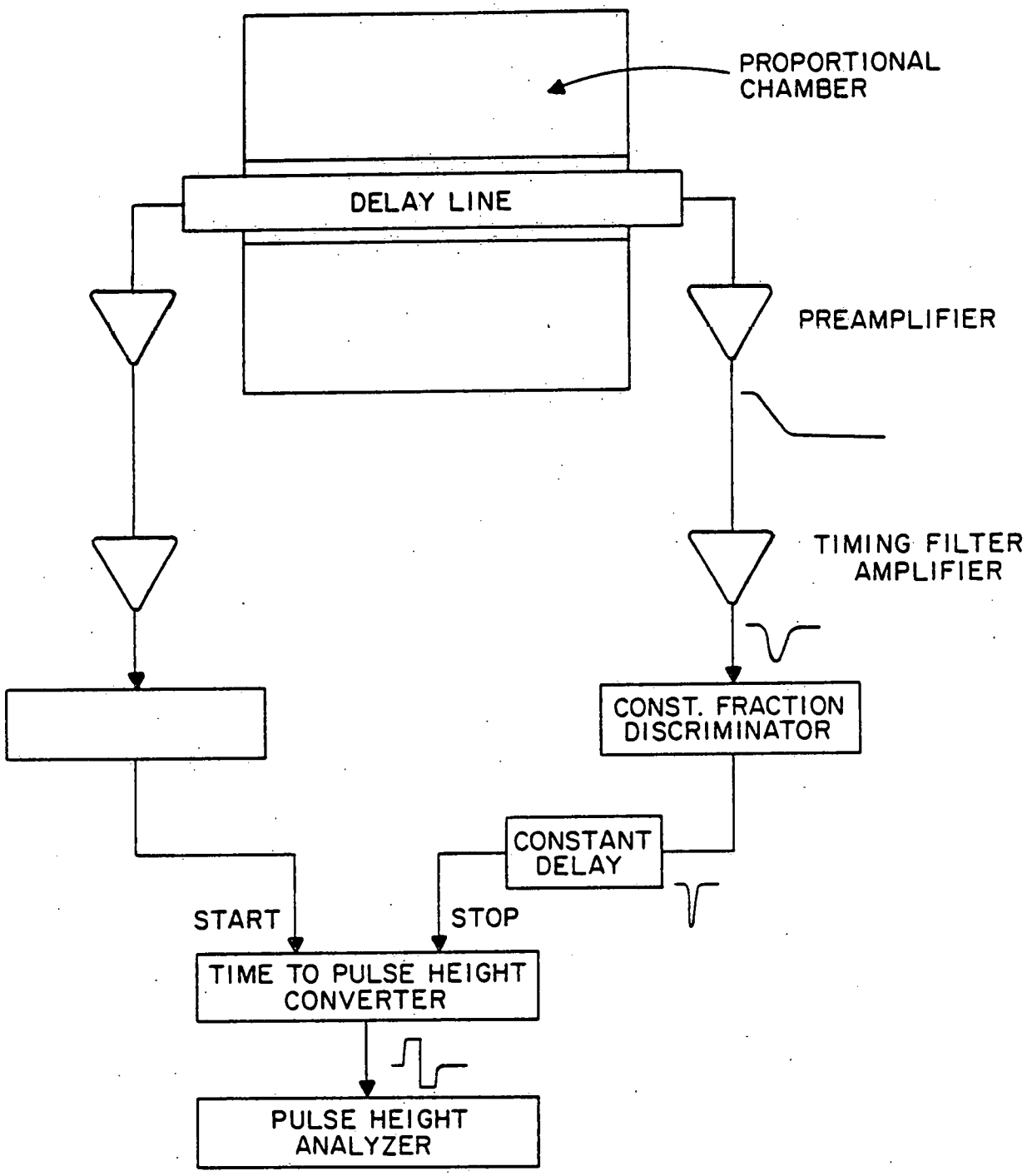
PROPORTIONAL CHAMBER
DELAY LINE
PREAMPLIFIER
TIMING FILTER AMPLIFIER
CONST. FRACTION DISCRIMINATOR
CONSTANT DELAY
START
STOP
TIME TO PULSE HEIGHT CONVERTER
PULSE HEIGHT ANALYZER

FIGURE 2

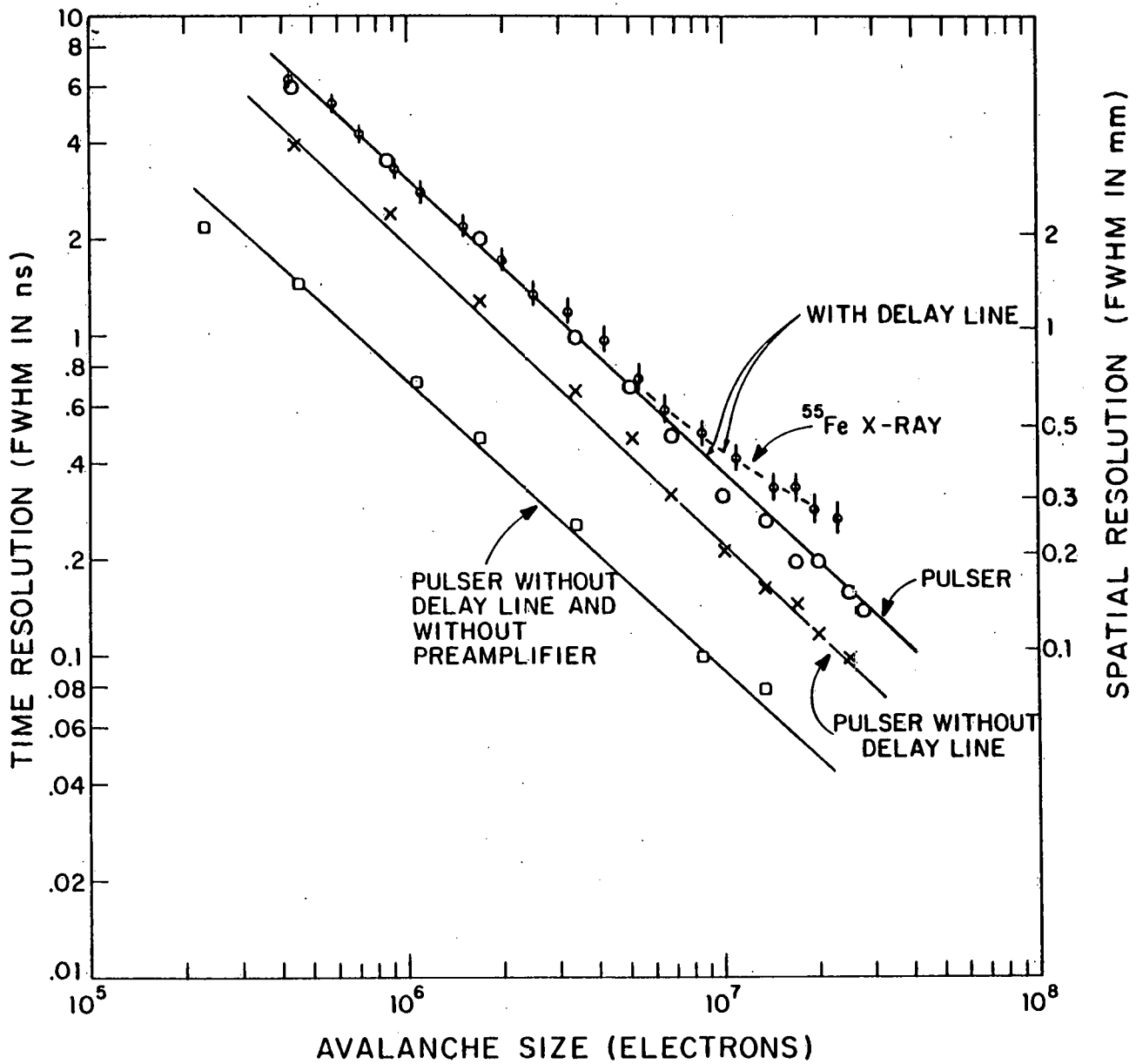
TIME RESOLUTION (FWHM IN ns)
SPATIAL RESOLUTION (FWHM IN mm)
AVALANCHE SIZE (ELECTRONS)
10
8
6
4
2
1
.8
.6
.4
.2
0.1
.08
.06
.04
.02
.01
10^5
10^6
10^7
10^8
2
1
0.5
0.3
0.2
0.1
WITH DELAY LINE
^{55}Fe X-RAY
PULSER
PULSER WITHOUT DELAY LINE AND WITHOUT PREAMPLIFIER
PULSER WITHOUT DELAY LINE

FIGURE 3

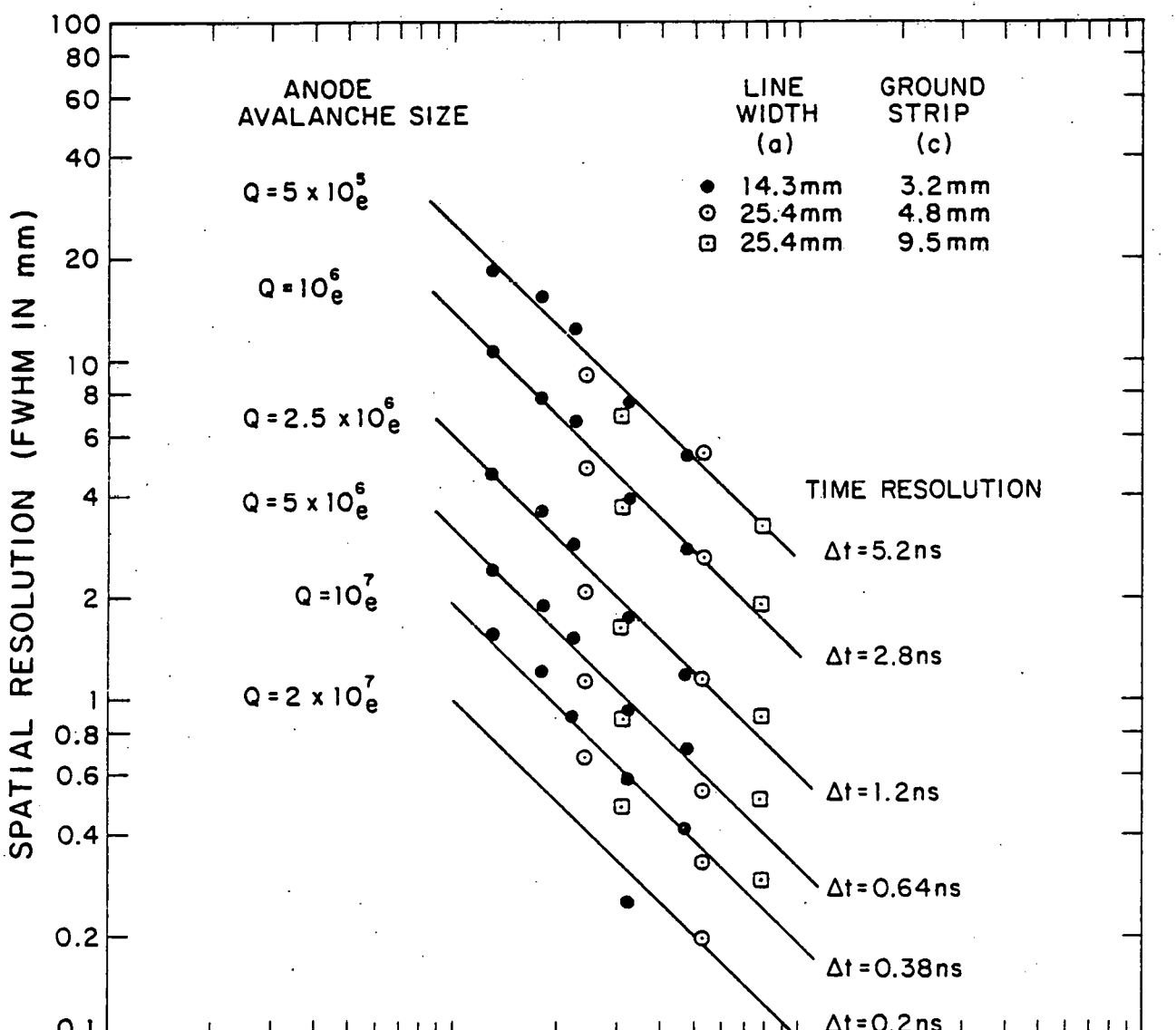
ANODE
AVALANCHE SIZE
LINE
WIDTH
(a)
GROUND
STRIP
(c)
14.3mm
3.2mm
25.4mm
4.8mm
25.4mm
9.5mm
Q = 5 x 10^5_e
Q = 10^6_e
Q = 2.5 x 10^6_e
Q = 5 x 10^6_e
Q = 10^7_e
Q = 2 x 10^7_e
TIME RESOLUTION
Δt = 5.2ns
Δt = 2.8ns
Δt = 1.2ns
Δt = 0.64ns
Δt = 0.38ns
Δt = 0.2ns
SPATIAL RESOLUTION (FWHM IN mm)
SPECIFIC LINE DELAY (ns/cm)
100
80
60
40
20
10
8
6
4
2
1
0.8
0.6
0.4
0.2
0.1
0.1
0.2
0.5
1
2
5
10
20
50
100

FIGURE 4

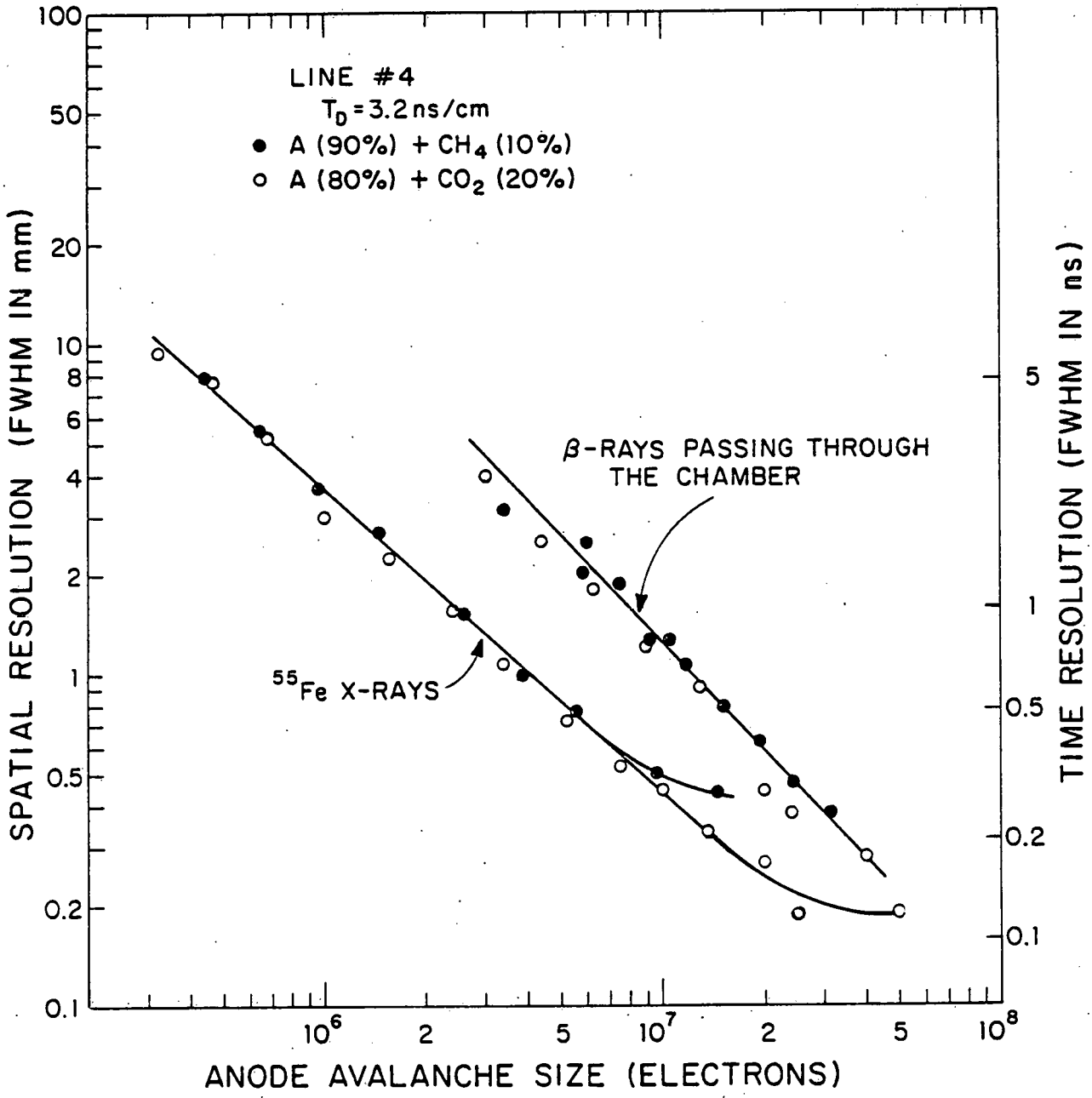
LINE #4
T_D = 3.2 ns/cm
● A (90%) + CH_4 (10%)
○ A (80%) + CO_2 (20%)
β-RAYS PASSING THROUGH THE CHAMBER
^{55}Fe X-RAYS
SPATIAL RESOLUTION (FWHM IN mm)
TIME RESOLUTION (FWHM IN ns)
ANODE AVALANCHE SIZE (ELECTRONS)
100
50
20
10
8
6
4
2
1
0.5
0.2
0.1
5
1
0.5
0.2
0.1
10^6
2
5
10^7
2
5
10^8

FIGURE 5

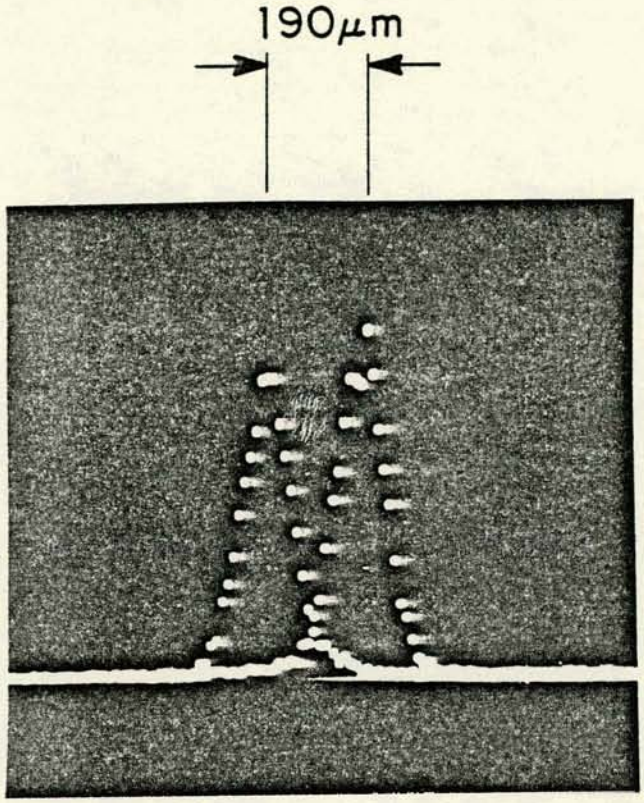

RESOLUTION:
~85μm FWHM

GAS: A + 20% CO_2

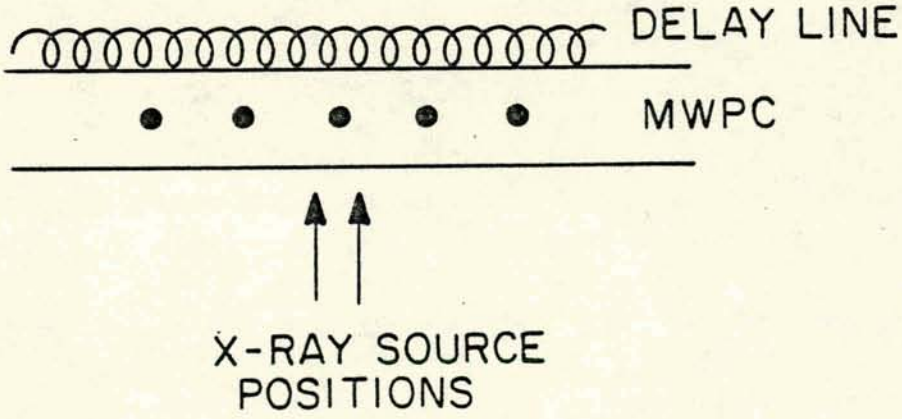

FIGURE 6